NANO LETTERS

pubs.acs.org/NanoLett Letter

Two-Dimensional-Dirac Surface States and Bulk Gap Probed via Quantum Capacitance in a Three-Dimensional Topological Insulator

Jimin Wang,* Cosimo Gorini, Klaus Richter, Zhiwei Wang, Yoichi Ando, and Dieter Weiss*

Cite This: https://dx.doi.org/10.1021/acs.nanolett.0c02733 Read Online

ACCESS | Metrics & More | Article Recommendations | Supporting Information

ABSTRACT: $BiSbTeSe_2$ is a 3D topological insulator (3D-TI) with Dirac type surface states and low bulk carrier density, as donors and acceptors compensate each other. Dominating low-temperature surface transport in this material is heralded by Shubnikov–de Haas oscillations and the quantum Hall effect. Here, we experimentally probe and model the electronic density of states (DOS) in thin layers of $BiSbTeSe_2$ by capacitance experiments both without and in quantizing magnetic fields. By probing the lowest Landau levels, we show that a large fraction of the electrons filled via field effect into the system ends up in (localized) bulk states and appears as a background DOS. The surprisingly strong temperature dependence of such background DOS can be traced back to Coulomb interactions. Our results point at the coexistence and intimate coupling of Dirac surface states with a bulk many-body phase (a Coulomb glass) in 3D-TIs.

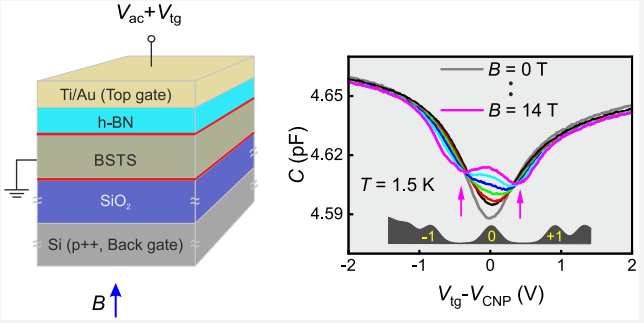

KEYWORDS: *compensated 3D-topological insulator, $BiSbTeSe_2$, quantum capacitance, Landau quantization, thermodynamic density of states, Coulomb glass*

Downloaded via UNIV REGENSBURG on November 19, 2020 at 12:42:11 (UTC).
See https://pubs.acs.org/sharingguidelines for options on how to legitimately share published articles.

INTRODUCTION

An ideal three-dimensional (3D) topological insulator (TI) is a band insulator, characterized by a gap in the single-particle energy spectrum, with symmetry protected conducting surface states[1,2] (and references therein). Experimentally available TIs like Bi_2Se_3 or Bi_2Te_3 are, however, far from ideal as they feature, due to intrinsic defects, a relatively high electron or hole density larger than 10^{18} cm^{-3} (see ref 3 and references therein). By combining p-type and n-type TI materials, that is, by compensation, the bulk concentration can be suppressed.[2,4] This comes at the price of large potential fluctuations at low temperatures as the resulting ionized donor and acceptor states are poorly screened and constitute a randomly fluctuating Coulomb potential, bending the band edges and creating electron and hole puddles.[5,6] These were observed by, for example, optical spectroscopy[3] and scanning tunneling experiments.[7] In the absence of metallic surface states, that is, in compensated conventional semiconductors, variable range hopping governs low-temperature transport ($T < 100$ K).[5,8] Recently, Skinner et al. have shown that the electronic density of states (DOS) in the bulk is nearly constant under these circumstances and features a Coulomb gap at the Fermi level.[5,6] In 3D-TIs, in addition Dirac surface states, which form a two-dimensional (2D) electron (hole) system, encase the bulk and constitute the dominating transport channel at low temperatures.

The nature of the surface and bulk phases is antithetical. The helical surface metal is an example of Berry Fermi liquid,[9] whose constituents are resilient to Anderson localization[1] and well described within a single (quasi-)particle picture. Bulk electrons on the other hand are topologically trivial and organize into a many-body disordered and localized phase. Indeed, such a phase shows characteristics[6,10] typically ascribed to a Coulomb glass, an exotic insulating state known and studied for decades yet far from being fully understood.[11−13] The interplay between these two different phases is a largely unexplored ground, one reason being the difficulty in engineering a system where both coexist. A largely compensated 3D-TI like $BiSbTeSe_2$ seems however ideally suited for this purpose, appearing as an intrinsic two-phase hybrid system. Moreover, understanding the surface-bulk interplay is not only interesting for fundamental reasons but also necessary if $BiSbTeSe_2$, and more generally (fully-) compensated 3D-TIs, is used as a device platform to realize, for example, topological superconductivity, Majorana zero modes,[14,15] and topological magnetoelectric effects.[16] With

Received: July 1, 2020
Revised: November 2, 2020

ACS Publications © XXXX American Chemical Society

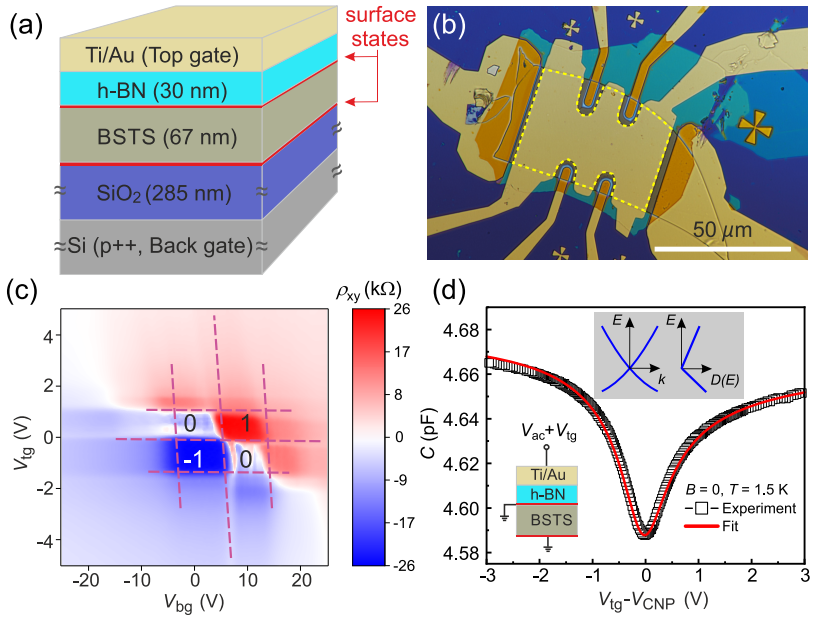

Figure 1. (a) Design of the layer sequence. Red lines sketch the topological surface states. (b) Optical micrograph of the device. The dashed yellow line marks the capacitor area of about 1.8×10^3 μm^2. (c) ρ_{xy} as a function of V_{tg} and V_{bg}, respectively, at T = 1.5 K and B = 14 T. The almost horizontal and vertical dashed purple lines separate the region of well-developed QHE with total filling factors of −1, 0, and 1 (unit h/e^2) from regions of higher filling factors. (d) $C(V)$ at T = 1.5 K and B = 0 T. Unlike graphene, the two branches are asymmetric with respect to CNP due to a nonlinear $E - k$ relation. The pronounced minimum reflects the bulk gap. For better comparison, the CNP of all measurements is shifted to zero via V_{CNP}. The red line is a fit using a Gaussian broadening of the Fermi level with σ = 29.4 meV (see text). To compare with experiment, we added a parasitic capacitance (mainly coming from wiring and bonding in the immediate vicinity of the device) of ∼3.07 pF. The lower left inset illustrates the measurement configuration, the upper inset shows the energy dispersion of the surface states in the bulk gap (left) and the corresponding DOS (right).

this goal in mind, we explore the surface-bulk interplay by probing the DOS of the Dirac surface states.

The method we used is capacitance spectroscopy, which provides complementary information, compared with common transport measurements. The total capacitance C, measured between a metallic top gate and the Dirac surface states, depends on the geometric capacitance, $C_0 = \epsilon\epsilon_0 A/d$, and the quantum capacitance $Ae^2D(\mu)$

$$C^{-1} = C_0^{-1} + [Ae^2D(\mu)]^{-1} \quad (1)$$

Here ϵ, d, and A are, respectively, relative dielectric constant, thickness of the insulator, and capacitor area, ϵ_0 is the vacuum dielectric constant, and $D(\mu)$ is the DOS at the Fermi level (chemical potential) μ. The quantum capacitance, connected in series to C_0, reflects the energy spectrum of 2D electron systems[17−19] and probes preferentially the top surface DOS in 3D-TIs.[20] At higher temperatures, $D(\mu)$ has to be replaced by the thermodynamic density of states (TDOS) at μ, $\mathcal{D}(\mu) = dn/d\mu$ with n as the carrier density. While gating of 3D-TIs and tuning of the carrier densities of top and bottom surfaces,[21−23] and even magnetocapacitance[23,24] has been explored in the past, the analysis of quantum capacitance and the DOS in a compensated TI like $BiSbTeSe_2$ remained uncharted. Our measurements show that although Dirac surface states dominate low-T transport as expected the bulk provides a background that is capable of absorbing a large amount of charge carriers. These missing charges are very common in 3D-TI transport experiments yet to the best of our knowledge are unexplained.[25−28] Furthermore, our in-depth analysis of the quantum capacitance data shows that the background is not a rigid object but reorganizes itself depending on the gate voltage (and temperature) value. This is a signature of a strongly interacting many-body phase, whose *effective* single-particle DOS reshapes itself adapting to varying conditions, for example, when charges are added or removed. The reshaping is typically slow, with a reaction/relaxation time which can be orders of magnitude slower than that of the surface Dirac metal. This provides evidence that $BiSbTeSe_2$ is not an ideal 3D-TI but rather a hybrid two-phase system and suggests that similar behavior should be expected for other compensated 3D-TI materials.

RESULTS AND DISCUSSION

Transport Measurements. The details of sample fabrication and measurements can be found in Supporting Information. Figure 1a,b displays the layer sequence and an optical micrograph of one of the devices, respectively. Temperature-dependent measurements show (see Figure S2 in Supporting Information) that at 1.5 K transport is entirely dominated by the surface with negligible contribution from the bulk. The carrier density and μ of top and bottom surfaces can be adjusted by top and bottom gate voltages, V_{tg}, V_{bg}, respectively. This is shown for the Hall resistivity at 14 T in Figure 1c. The device displays well-developed quantum Hall plateaus at total filling factor ν = −1, 0, and 1 (note that for each Dirac surface state, Landau levels are fully filled at half integer ν and total filling factor 1, corresponding to ν = 1/2 on top and bottom surfaces.[25]). The plateaus are well separated from each other and marked by dashed purple lines. As these lines run nearly parallel to the V_{tg}- and V_{bg}-axes, respectively, we conclude that the carrier density on top and bottom can be tuned nearly independently.

Capacitance Measurements. Figure 1d shows the measured capacitance C, which is directly connected to the

https://dx.doi.org/10.1021/acs.nanolett.0c02733
Nano Lett. XXXX, XXX, XXX−XXX

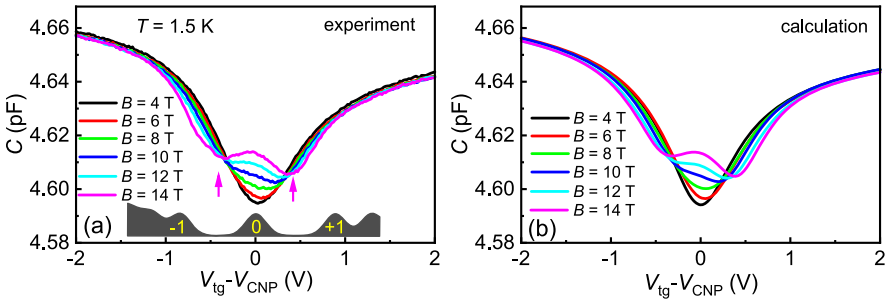

Figure 2. (a) $C(V_{tg})$ for B ranging from 4 to 14 T. The lower inset sketches the LL DOS for LLs −1, 0, and 1. Arrows mark the position of the Landau gaps for the 14 T trace. (b) Model calculations to (a) based on eq 3 after adding a parasitic capacitance of ∼3.06 pF. Parameters of the fit at 1.5 K: Γ = 14.9−15.9 meV; $D_b = 2.4 \times 10^{35}$ m^{-2} J^{-1}. Although the position of the 0th LL changes slightly with B, we use the same zero-field value V_{CNP} for all curves.

DOS, see eq 1 (measurement details are in Supporting Information). The measured trace with a minimum at the Dirac or charge neutrality point (CNP) resembles the quantum capacitance measured for graphene, apart from a pronounced electron−hole asymmetry[19,29,30] due to a parabolic contribution to the linear $E(k)$ dispersion.[31] Explicitly, the latter reads $E = \pm\hbar v_F k + \frac{\hbar^2 k^2}{2m^*}$ where $\hbar$ is the reduced Planck constant, v_F is the Fermi velocity at the Dirac point, and m^* is the effective mass. It is sketched in the upper inset of Figure 1d, together with the electron−hole asymmetric, nearly E-linear DOS, given by $D(E) = \left|\frac{m^*(\Omega - m^* v_F)}{2\pi\hbar^2\Omega}\right|$. Here we used that $k = \sqrt{4\pi|n|}$ and $\Omega = \sqrt{(m^* v_F)^2 + 2Em^*}$.

While in a perfect system $D(E)$ vanishes at the CNP, disorder smears the singularity, as in case of graphene.[19] We model the potential fluctuations by a Gaussian distribution of energies with width σ, resulting in an average DOS $\langle D(\mu)\rangle = \int_{-\infty}^{\infty} D(E)\frac{1}{\sqrt{2\pi}\sigma}\exp\left[\frac{-(E-\mu)^2}{2\sigma^2}\right]dE$. To convert energies into voltages we use $n = C_0(V_{tg} - V_0)/(Ae)$ with e the elementary charge and V_0 describing n at zero voltage. By fitting $\langle D(\mu)\rangle$ to the data in Figure 1d, we extract σ = 29.4 meV, $v_F = 3.2 \times 10^5$ m/s, and $m^* = 0.47m_0$ (m_0 = free electron mass). The broadening σ, which is in reasonable agreement with theory,[32] is only important in the immediate vicinity of the CNP but hardly affects the values of v_F and m^*. The obtained v_F and m^* values agree well with ARPES data[21,33] and values extracted from Shubnikov−de Haas oscillations.[31]

***B*-Field Dependence of Capacitance Measurements.** Our key result arises when we crank up the magnetic field and measure signatures of the Landau level (LL) spectrum, shown in Figure 2a. At the 0th LL level position, a local maximum emerges with increasing B-field, flanked by minima at each side. The two minima, highlighted by arrows, correspond to the Landau gaps between LLs 0 and ±1 (see Figure 2a). Because of the large broadening, higher LLs do not get resolved. Lowering T down to 50 mK does not resolve more structure, indicating that disorder broadening is the limiting factor. By sweeping V_{tg} across the 0th LL, that is, from arrow position to arrow position, the carrier density changes by the LL degeneracy $\Delta n = eB/h$. In contrast, the change of carrier density Δn, calculated via capacitance, $\Delta n = \frac{C_0}{Ae}\Delta V_{tg}$, is by a factor of 1.4 higher. Hence, we must assume that a large fraction of the carriers, induced by field effect, ends up in the bulk and is localized at low T.

To compare with these experiments we calculate $C(V_{tg})$ using Gaussian-broadened LLs $D_{LL}(E) = \frac{1}{\sqrt{2\pi}\Gamma}\frac{eB}{h}\sum\exp\left[\frac{-(E-E_n)^2}{2\Gamma^2}\right]$ with broadening Γ. The LL spectrum dispersion reads[34]

$$E_n = |n|\frac{\hbar eB}{m^*} + \mathrm{sgn}(n)\sqrt{\left(\frac{\hbar eB}{2m^*}\right)^2 + 2eB\hbar v_F^2|n|} \quad (2)$$

with $n = 0, \pm1, \pm2, \ldots$, and the tiny Zeeman splitting was neglected. Using the above DOS is insufficient to describe the data: the calculated distance ΔV_{tg} between adjacent Landau gaps is too small and does not match the minima positions observed in experiment (marked by arrows in Figure 2a for the 14 T trace, see Figure S4 in Supporting Information as an example). ΔV_{tg} is the voltage needed to fully fill the 0th LL of the surface states. Because ΔV_{tg} in experiment is larger than that in calculation (relies on the filling rate $dn/dV_{tg} \approx C_0/(Ae)$), it means that a fraction of the field-induced electrons does not go to the surface states but eventually into the bulk. Thus, a higher voltage (higher δn) is needed to fill the zeroth LL. In contrast, we obtain almost perfect agreement, see Figure 2b, if we introduce an energy-independent background DOS D_b which models these bulk states. The calculated TDOS we compare with experiment thus reads

$$\mathcal{D}(\mu) = \int_{-\infty}^{\infty}[D_{LL}(E) + D_b]\frac{\partial f}{\partial\mu}\,dE \quad (3)$$

with $f = f(E - \mu, T)$ as the Fermi function.

As shown in Figure 2b, the constant background D_b leads to excellent agreement with experiment. Although the bulk DOS is hardly directly accessible by the quantum capacitance itself (i.e., by its value), we probe it indirectly via the missing charge carriers given by the Landau gap positions. This missing charge carrier issue holds also for the quantum Hall trace in Figure 1c where ∼30% of the induced electrons are missing. Indeed, it also appears in several other publications with missing electron fractions ranging from 30% (as here) to 75% (see refs 25−28).

The bottom line is the following: The change of surface carrier density extracted from the Landau gap positions is smaller than the one "loaded" into the system within the same voltage interval. Further, the filling rate dn/dV_{tg} determined by the classical Hall effect at 1.5 K is consistent with the one found for the surface states (see Supporting Information). Thus, the charge carriers loaded at low T into the bulk are localized and do not contribute to transport. This is consistent

https://dx.doi.org/10.1021/acs.nanolett.0c02733
Nano Lett. XXXX, XXX, XXX−XXX

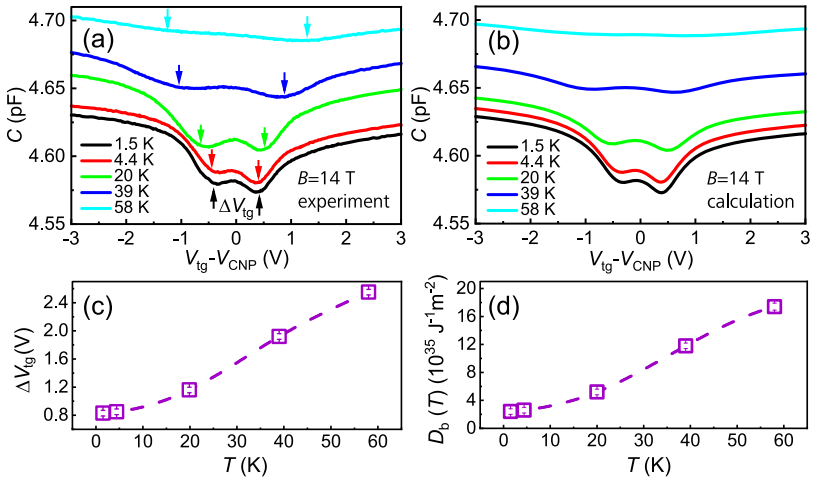

Figure 3. (a) $C(V_{tg})$ at B = 14 T for various Ts. Arrows mark the minima corresponding to Landau gaps. For increasing T, the voltage difference ΔV_{tg} between adjacent gaps increases. The trace at 1.5 K was shifted down by 0.032 pF for clarity. (b) Calculated $C(V_{tg})$ using eq 3 with D_b values in (d), and Γ = 13 to 15.2 meV. A nearly T-independent parasitic capacitance of 3.06 ± 0.04 pF is used to best fit the data. (c) ΔV_{tg} versus T. (d) Extracted D_b. The dashed lines in (c,d) are guides to the eye.

with transport experiments[25,35] and also in line with what is expected in compensated semiconductors,[8] as was recently highlighted in ref 5. There, bulk transport of compensated TI was considered, where local puddles of n- and p-regions form. In this regime, low-T transport is governed by variable range hopping, and the DOS is, apart from the Coulomb gap, essentially constant for perfect compensations but changes its form strongly if the chemical potential shifts.[5,6,8]

Using a constant background affects somewhat the values extracted above from $C(V_{tg}, B = 0)$. Thus, we fitted the trace in Figure 1d using the same $D_b = 2.4 \times 10^{35}$ m^{-2} J^{-1}. Now a reduced broadening σ = 15 meV is needed, which is still in reasonable agreement with theory.[32] $C(V_{tg})$ is then best described by slightly modified values: $v_F = 2.8 \times 10^5$ m/s and $m^* = 0.57m_0$, respectively, still compatible with results reported elsewhere.[21,31,33]

Temperature Dependence of Quantum Capacitance. The background DOS rises quickly with temperature. Corresponding $C(V_{tg})$ data for 14 T and various Ts up to 58 K are shown in Figure 3a. The local minima due to Landau gaps, marked by arrows, shift with increasing T to larger V_{tg}. The corresponding $\Delta V_{tg}(T)$ is shown in Figure 3c. For fixed B, the Landau degeneracy eB/h is constant and does not depend on temperature. The increasing ΔV_{tg} needed to fill the 0th LL of the surface states thus indicates that with increasing T more carriers are lost to the bulk. Similar behavior was found for quantum Hall data.[25,35] Clearly, to model the Landau gap positions correctly a strongly T-dependent thermodynamic density of states (TDOS) is required. A simple approach consists of introducing a T-dependent background DOS, $D_b \rightarrow D_b(T)$. Its values used to fit the data of Figure 3a are shown in Figure 3d; the resulting $C(V_{tg})$ traces for different temperatures are plotted in Figure 3b. D_b is nearly constant at low T but rises quickly at higher temperatures, as shown in Figure 3d. However, a closer inspection of the possible microscopic origins of $D_b(T)$ reveals the central issue hiding behind our data: How can the TDOS near the Dirac point (at 14 T the Landau gaps are located between −30 and +30 meV, as estimated by eq 2) be at the same time practically flat, yet so strongly T-dependent? One could attempt to explain its constant value at 1.5 K by conventional trapped surface states between BSTS and hBN. They are likely responsible for the small hysteresis observed when sweeping V_{tg}, but the $C-V$ trace shift for up- and down-sweep first stays constant at low T, then drops with increasing temperature (see the Supporting Information). This rules out the interface states as reason for the striking TDOS increase with T. Alternatively, one could argue that the increased TDOS stems from thermal smearing of the DOS of the (effective) band edges, separated by a reduced gap of ∼60 meV, as determined by the measured activation energy (see Supporting Information), instead of the full gap of 300 meV. Modeling this scenario by choosing the DOS at the band edges such that the average TDOS, when sweeping μ from one Landau gap to the other, equals the extracted constant D_b cannot explain the experimental traces: The resulting TDOS is strongly energy-dependent, reflecting the sharp DOS shoulders at the band edges, and this strong dependence would completely dominate the capacitance signal (Figure S10 in Supporting Information). Thus, we are unable to find a single-particle DOS which is consistent with the experimental findings, suggesting that a single-particle picture is simply not adequate.

Probing the Many-Body Background. A way out of this apparent dead-end is provided by the strongly fluctuating potential landscape of compensated TIs like $BiSbTeSe_2$, sketched in Figure 4a,b, where Coulomb interaction dominates.[5] In a nutshell, the background DOS emerges as an *effective* single particle DOS describing the ensemble of strongly interacting electrons filling bulk impurity states.[8] As such, it is actually a μ- and T-dependent object, $D_b \rightarrow D_b(E, \mu, T)$, which in particular can massively reshape itself when μ is varied,[6] see Figure 4a,b. The reshaping is a complex many-body problem and can be very slow.[13,36] The situation is further complicated by the presence of the Dirac surface states encasing the bulk. Because precise time scales for $BiSbTeSe_2$ are not known and a comprehensive theory covering all aspects of our 3D TI scenario is not available, we can only argue along phenomenological lines. First, the time scale of about 1 min needed to produce each data point after changing V_{tg} is assumed sufficiently long for the reshaping to take place, at least partially. Second, we look for a bare-bone DOS toy model meeting three fundamental constraints: (i) the resulting TDOS

https://dx.doi.org/10.1021/acs.nanolett.0c02733
Nano Lett. XXXX, XXX, XXX−XXX

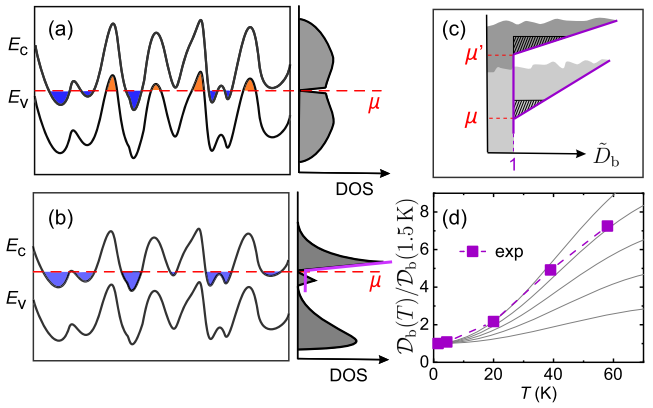

Figure 4. (a) Conduction (E_c) and valence band (E_v) profiles, fluctuating due to long-range Coulomb interactions for perfect compensation. Electron- and hole puddles form. A sketch of the symmetric bulk DOS including the Coulomb gap at μ is shown at right.[5] (b) For nonperfect compensation, for example, for the donor concentration slightly higher than the one of acceptors, the fluctuation amplitude and the shape of the many particle DOS, sketched following ref 6 change considerably. We expect a similar situation for changing the gate voltage instead of compensation. Note that the overall number of impurity states (shaded region at right) is fixed and independent of the shape. For modeling we use the purple shape of the DOS, ignoring the Coulomb gap at μ. (c) DOS of our toy model mimicking the DOS of (b) (purple line). The hatched areas illustrate the origin of the TDOS temperature dependence. (d) Solid gray lines represent the calculated TDOS of our toy model with the parameter a varying from 10 (bottom) to 50 (top) in steps of 10. Filled squares are experimental data. All curves (data points) are normalized to their values at T = 1.5 K.

is everywhere constant but strongly T-dependent; (ii) the overall number of charges lost to the bulk when scanning V_{tg} from one Landau gap to the other increases by a factor of roughly 8 in the interval T = 1.5 K to T = 58 K; (iii) its shape is qualitatively compatible with established theoretical results.[6] Consider therefore the TDOS

$$\mathcal{D}_b(\mu) = \int \partial_\mu [D_b(E, \mu) f(E - \mu, T)] dE \tag{4}$$

the μ-derivative acting on both the Fermi function f and D_b. The background DOS is given by a toy model (We do not consider an explicit T-dependence of the DOS as too little precise knowledge is available for a meaningful guess. Note also that we ignore the presence of a Coulomb gap.[8,10,37−41] This is because the gap is a function of $E - \mu$, not of μ alone, and thus its contribution to $\partial n/\partial\mu$ can be neglected, at least within our phenomenological approach; see Supporting Information):

$$\tilde{D}(E, \mu) \equiv \frac{D_b(E, \mu)}{D_0} = \begin{cases} 1 & \text{if} \quad E_m^* < E \le \mu \\ [1 + a\mu(E - \mu)] & \text{if} \quad \mu < E < E_M^* \end{cases} \tag{5}$$

Here, D_0 is the TDOS value measured at T = 0, a is a parameter, while E_m^*, E_M^* are cutoff energies such that $|E_m^* - \mu_1|$, $|E_M^* - \mu| \gg k_B T_{max}$ with μ_1 being the position of the lower Landau gap and T_{max} = 58 K (see corresponding sketch in Figure S11 in Supporting Information). Beyond such cut-offs the form of $D_b(E, \mu)$ is irrelevant for computing the corresponding TDOS. The dimensionless $\tilde{D}_b(E, \mu)$ is sketched in Figure 4c for two different values of μ. Notice that such a DOS is the result of a reorganization of impurity states not of the appearance of additional states. That is, it is constrained by the condition that the overall number of donors and acceptors states within the gap is fixed. Thus, its profile above μ sharpens because impurity states from higher energies migrate closer to the chemical potential as the latter increases, while it stays flat below μ as it represents only the average value of the DOS in the region $E_m^* < E \le \mu$ (see sketch in Figure 4c and Figure S11 in Supporting Information). In other words, consider two values of the chemical potential $\mu' > \mu$, both within the energy region defined by the position of the lower (μ_1) and upper Landau gap (μ_2). The DOS reorganization is such that more higher energy states are available within $k_B T$ of μ' than within $k_B T$ of μ, see hatched areas in Figure 4c, and this difference is responsible for a strongly T-dependent TDOS (see Supporting Information). Thus, the overall amount of charges lost to the bulk between $\mu = \mu_2$ and $\mu = \mu_1$ is

$$\delta n_b = \int D_b(E, \mu_2) f(E - \mu_2, T) dE - \int D_b(E, \mu_1) f(E - \mu_1, T) dE \tag{6}$$

As discussed above, this quantity cannot be written as $\int D_b^{rigid}(E)[f(E - \mu_2) - f(E - \mu_1)]dE$, in terms of a rigid single-particle DOS $D_b^{rigid}(E)$. In Figure 4d, we compare the measured TDOS normalized to its T = 1.5 K value, $\mathcal{D}_b(T)/\mathcal{D}_b(1.5\,K)$ and the one computed from eqs 4 and 5. Qualitatively, the similarity is evident. We emphasize however that our toy model can only be taken as an empirical guide to the data.

CONCLUSIONS

By probing the capacitance of a $BiSbTeSe_2$ capacitor structure we are able to extract the electronic DOS as a function of the gate voltage (chemical potential μ). Our experimental data, together with the calculations, show that the filling (via field-effect) of Dirac surface states and conventional bulk states is closely intertwined. While we observe the Landau quantization of the Dirac surface states in the quantum capacitance signal, the position of the Landau gaps and their increased separation on the gate voltage scale with increasing temperature can only be understood by considering bulk states. These experiments provide a so far unknown method to investigate the many-particle DOS of the bulk of a highly compensated TI. We find the corresponding bulk TDOS to be constant as a function of μ but strongly temperature dependent. This result is incompatible with a single-particle picture and is evidence of the many-body character of the bulk phase. Indeed, the in-depth analysis of quantum capacitance data suggests that the background density of states reorganizes whenever the gate voltage (chemical potential) is changed, on the time scale of a minute. This is compatible with the slow (glassy) dynamics of a disordered and strongly interacting phase,[10,13] as expected in the bulk of a compensated TI.[3,6,7] To the best of our knowledge, the dynamics of such a surface-bulk two-phase hybrid system is largely uncharted ground at the moment. However, a proper understanding of it is crucial for potential device concepts based on the properties of topological surface states.

ASSOCIATED CONTENT

Supporting Information

The Supporting Information is available free of charge at https://pubs.acs.org/doi/10.1021/acs.nanolett.0c02733.

https://dx.doi.org/10.1021/acs.nanolett.0c02733
Nano Lett. XXXX, XXX, XXX−XXX

Details of sample fabrication, transport, and capacitance measurements; resistivity-temperature relation; determining ΔV_{tg}; failure of fitting $C-V$ trace at 14 T without background DOS; transport data and estimating the filling rate from Hall measurements; comparing fitting of $C-V$ at B = 0 T and T = 1.5 K with and without background DOS; extracting the quantum capacitance from $C(V)$ curves; does the strong temperature dependence of the TDOS come from a single particle gap?; details on the DOS toy model; discussion on frequency dependence; discussion on hysteresis (PDF)

AUTHOR INFORMATION

Corresponding Authors

Jimin Wang − *Institute of Experimental and Applied Physics, University of Regensburg, 93040 Regensburg, Germany*; Email: jimin.wang@physik.uni-regensburg.de

Dieter Weiss − *Institute of Experimental and Applied Physics, University of Regensburg, 93040 Regensburg, Germany*; Email: dieter.weiss@physik.uni-regensburg.de

Authors

Cosimo Gorini − *Institute of Theoretical Physics, University of Regensburg, 93040 Regensburg, Germany*

Klaus Richter − *Institute of Theoretical Physics, University of Regensburg, 93040 Regensburg, Germany*

Zhiwei Wang − *Physics Institute II, University of Cologne, 50937 Köln, Germany; Key Laboratory of Advanced Optoelectronic Quantum Architecture and Measurement, Ministry of Education, School of Physics, Beijing Institute of Technology, Beijing 100081, China*

Yoichi Ando − *Physics Institute II, University of Cologne, 50937 Köln, Germany*

Complete contact information is available at: https://pubs.acs.org/10.1021/acs.nanolett.0c02733

Author Contributions

Z.W. and Y.A. synthesized the crystals. D.W. and J.W. designed the experiments. J.W. fabricated the devices, performed the transport and capacitance measurements. C.G. and K.R. conducted the theory. J.W., C.G., and D.W analyzed the data and wrote the paper from inputs from other coauthors.

Notes

The authors declare no competing financial interest.

ACKNOWLEDGMENTS

We thank F. Evers for inspiring discussions, and G. Vignale for a careful reading of the manuscript. The work at Regensburg was funded by the Deutsche Forschungsgemeinschaft (DFG, German Research Foundation), Project-ID 314695032 - CRC 1277 (Subprojects A07, A08). This project has received further funding from the European Research Council (ERC) under the European Union's Horizon 2020 research and innovation programme (Grant Agreement 787515, ProMotion), as well as the Alexander von Humboldt Foundation. The work at Cologne was funded by the Deutsche Forschungsgemeinschaft (DFG, German Research Foundation), Project number 277146847 - CRC 1238 (Subproject A04).

REFERENCES

(1) Hasan, M. Z.; Kane, C. L. Colloquium: Topological insulators. *Rev. Mod. Phys.* **2010**, *82*, 3045−3067.

(2) Ando, Y. Topological Insulator Materials. *J. Phys. Soc. Jpn.* **2013**, *82*, 102001.

(3) Borgwardt, N.; Lux, J.; Vergara, I.; Wang, Z.; Taskin, A. A.; Segawa, K.; van Loosdrecht, P. H. M.; Ando, Y.; Rosch, A.; Grüninger, M. Self-organized charge puddles in a three-dimensional topological material. *Phys. Rev. B: Condens. Matter Mater. Phys.* **2016**, *93*, 245149.

(4) Ren, Z.; Taskin, A. A.; Sasaki, S.; Segawa, K.; Ando, Y. Optimizing $Bi_{2-x}Sb_xTe_{3-y}Se_y$ solid solutions to approach the intrinsic topological insulator regime. *Phys. Rev. B: Condens. Matter Mater. Phys.* **2011**, *84*, 165311.

(5) Skinner, B.; Chen, T.; Shklovskii, B. I. Why Is the Bulk Resistivity of Topological Insulators So Small? *Phys. Rev. Lett.* **2012**, *109*, 176801.

(6) Skinner, B.; Chen, T.; Shklovskii, B. I. Effects of bulk charged impurities on the bulk and surface transport in three-dimensional topological insulators. *J. Exp. Theor. Phys.* **2013**, *117*, 579−592.

(7) Knispel, T.; Jolie, W.; Borgwardt, N.; Lux, J.; Wang, Z.; Ando, Y.; Rosch, A.; Michely, T.; Grüninger, M. Charge puddles in the bulk and on the surface of the topological insulator $BiSbTeSe_2$ studied by scanning tunneling microscopy and optical spectroscopy. *Phys. Rev. B: Condens. Matter Mater. Phys.* **2017**, *96*, 195135.

(8) Efros, A. L.; Shklovskii, B. I. *Electronic Properties of Doped Semiconductors*; Springer-Verlag: New York, 1984; http://www.tpi.umn.edu/shklovskii.

(9) Chen, J. Y.; Son, D. T. Berry Fermi liquid theory. *Ann. Phys. (Amsterdam, Neth.)* **2017**, *377*, 345.

(10) Meroz, Y.; Oreg, Y.; Imry, Y. Memory effects in the electron glass. *EPL* **2014**, *105*, 37010.

(11) Davies, J. H.; Lee, P. A.; Rice, T. M. Properties of the electron glass. *Phys. Rev. B: Condens. Matter Mater. Phys.* **1984**, *29*, 4260.

(12) Vignale, G. Quantum electron glass. *Phys. Rev. B: Condens. Matter Mater. Phys.* **1987**, *36*, 8192.

(13) Ovadyahu, Z. Interacting Anderson insulators: The intrinsic electron glass. *C. R. Phys.* **2013**, *14*, 700.

(14) Fu, L.; Kane, C. L. Superconducting Proximity Effect and Majorana Fermions at the Surface of a Topological Insulator. *Phys. Rev. Lett.* **2008**, *100*, 096407.

(15) Fu, L.; Kane, C. L. Josephson current and noise at a superconductor/quantum-spin-Hall-insulator/superconductor junction. *Phys. Rev. B: Condens. Matter Mater. Phys.* **2009**, *79*, 161408.

(16) Essin, A. M.; Moore, J. E.; Vanderbilt, D. Magnetoelectric Polarizability and Axion Electrodynamics in Crystalline Insulators. *Phys. Rev. Lett.* **2009**, *102*, 146805.

(17) Smith, T. P.; Goldberg, B. B.; Stiles, P. J.; Heiblum, M. Direct measurement of the density of states of a two-dimensional electron gas. *Phys. Rev. B: Condens. Matter Mater. Phys.* **1985**, *32*, 2696−2699.

(18) Mosser, V.; Weiss, D.; Klitzing, K.; Ploog, K.; Weimann, G. Density of states of GaAs-AlGaAs-heterostructures deduced from temperature dependent magnetocapacitance measurements. *Solid State Commun.* **1986**, *58*, 5−7.

(19) Ponomarenko, L. A.; Yang, R.; Gorbachev, R. V.; Blake, P.; Mayorov, A. S.; Novoselov, K. S.; Katsnelson, M. I.; Geim, A. K. Density of States and Zero Landau Level Probed through Capacitance of Graphene. *Phys. Rev. Lett.* **2010**, *105*, 136801.

(20) Kozlov, D. A.; Bauer, D.; Ziegler, J.; Fischer, R.; Savchenko, M. L.; Kvon, Z. D.; Mikhailov, N. N.; Dvoretsky, S. A.; Weiss, D. Probing Quantum Capacitance in a 3D Topological Insulator. *Phys. Rev. Lett.* **2016**, *116*, 166802.

(21) Fatemi, V.; Hunt, B.; Steinberg, H.; Eltinge, S. L.; Mahmood, F.; Butch, N. P.; Watanabe, K.; Taniguchi, T.; Gedik, N.; Ashoori, R. C.; Jarillo-Herrero, P. Electrostatic Coupling between Two Surfaces of a Topological Insulator Nanodevice. *Phys. Rev. Lett.* **2014**, *113*, 206801.

(22) Xiong, J.; Khoo, Y.; Jia, S.; Cava, R. J.; Ong, N. P. Tuning the quantum oscillations of surface Dirac electrons in the topological insulator Bi_2Te_2Se by liquid gating. *Phys. Rev. B: Condens. Matter Mater. Phys.* **2013**, *88*, No. 035128.

(23) Chong, S. K.; Han, K. B.; Sparks, T. D.; Deshpande, V. V. Tunable Coupling between Surface States of a Three-Dimensional Topological Insulator in the Quantum Hall Regime. *Phys. Rev. Lett.* **2019**, *123*, 036804.
(24) Chong, S. K.; Tsuchikawa, R.; Harmer, J.; Sparks, T. D.; Deshpande, V. V. Landau Levels of Topologically-Protected Surface States Probed by Dual-Gated Quantum Capacitance. *ACS Nano* **2020**, *14*, 1158−1165.
(25) Xu, Y.; Miotkowski, I.; Chen, Y. P. Quantum transport of two-species Dirac fermions in dual-gated three-dimensional topological insulators. *Nat. Commun.* **2016**, *7*, 11434.
(26) Zhang, S.; Pi, L.; Wang, R.; Yu, G.; Pan, X.-C.; Wei, Z.; Zhang, J.; Xi, C.; Bai, Z.; Fei, F.; Wang, M.; Liao, J.; Li, Y.; Wang, X.; Song, F.; Zhang, Y.; Wang, B.; Xing, D.; Wang, G. Anomalous quantization trajectory and parity anomaly in Co cluster decorated BiSbTeSe2 nanodevices. *Nat. Commun.* **2017**, *8*, 977.
(27) Chong, S. K.; Han, K. B.; Nagaoka, A.; Tsuchikawa, R.; Liu, R.; Liu, H.; Vardeny, Z. V.; Pesin, D. A.; Lee, C.; Sparks, T. D.; Deshpande, V. V. Topological Insulator-Based van der Waals Heterostructures for Effective Control of Massless and Massive Dirac Fermions. *Nano Lett.* **2018**, *18*, 8047−8053.
(28) Yoshimi, R.; Tsukazaki, A.; Kozuka, Y.; Falson, J.; Takahashi, K. S.; Checkelsky, J. G.; Nagaosa, N.; Kawasaki, M.; Tokura, Y. Quantum Hall effect on top and bottom surface states of topological insulator (Bi1-xSbx)2Te3 films. *Nat. Commun.* **2015**, *6*, 6627.
(29) Yu, G. L.; Jalil, R.; Belle, B.; Mayorov, A. S.; Blake, P.; Schedin, F.; Morozov, S. V.; Ponomarenko, L. A.; Chiappini, F.; Wiedmann, S.; Zeitler, U.; Katsnelson, M. I.; Geim, A. K.; Novoselov, K. S.; Elias, D. C. Interaction phenomena in graphene seen through quantum capacitance. *Proc. Natl. Acad. Sci. U. S. A.* **2013**, *110*, 3282−3286.
(30) Xia, J.; Chen, F.; Li, J.; Tao, N. Measurement of the quantum capacitance of graphene. *Nat. Nanotechnol.* **2009**, *4*, 505.
(31) Taskin, A. A.; Ren, Z.; Sasaki, S.; Segawa, K.; Ando, Y. Observation of Dirac Holes and Electrons in a Topological Insulator. *Phys. Rev. Lett.* **2011**, *107*, 016801.
(32) Skinner, B.; Shklovskii, B. I. Theory of the random potential and conductivity at the surface of a topological insulator. *Phys. Rev. B: Condens. Matter Mater. Phys.* **2013**, *87*, No. 075454.
(33) Arakane, T.; Sato, T.; Souma, S.; Kosaka, K.; Nakayama, K.; Komatsu, M.; Takahashi, T.; Ren, Z.; Segawa, K.; Ando, Y. Tunable Dirac cone in the topological insulator Bi2-xSbxTe3-ySey. *Nat. Commun.* **2012**, *3*, 636.
(34) Taskin, A. A.; Ando, Y. Berry phase of nonideal Dirac fermions in topological insulators. *Phys. Rev. B: Condens. Matter Mater. Phys.* **2011**, *84*, No. 035301.
(35) Xu, Y.; Miotkowski, I.; Liu, C.; Tian, J.; Nam, H.; Alidoust, N.; Hu, J.; Shih, C.-K.; Hasan, M. Z.; Chen, Y. P. Observation of topological surface state quantum Hall effect in an intrinsic three-dimensional topological insulator. *Nat. Phys.* **2014**, *10*, 956.
(36) Amir, A.; Oreg, Y.; Imry, Y. Electron Glass Dynamics. *Annu. Rev. Condens. Matter Phys.* **2011**, *2*, 235.
(37) Grunewald, M.; Pohlmann, B.; Schweitzer, L.; Wurtz, D. Mean field approach to the electron glass. *J. Phys. C: Solid State Phys.* **1982**, *15*, L1153.
(38) Mogilyanskii, A. A.; Raikh, M. Self-consistent description of Coulomb gap at finite temperatures. *J. Exp. Theor. Phys.* **1989**, *68*, 1081.
(39) Sandow, B.; Gloos, K.; Rentzsch, R.; Ionov, A. N.; Schirmacher, W. Electronic Correlation Effects and the Coulomb Gap at Finite Temperature. *Phys. Rev. Lett.* **2001**, *86*, 1845−1848.
(40) Vaknin, A.; Ovadyahu, Z.; Pollak, M. Nonequilibrium field effect and memory in the electron glass. *Phys. Rev. B: Condens. Matter Mater. Phys.* **2002**, *65*, 134208.
(41) Bardalen, E.; Bergli, J.; Galperin, Y. M. Coulomb glasses: A comparison between mean field and Monte Carlo results. *Phys. Rev. B: Condens. Matter Mater. Phys.* **2012**, *85*, 155206.

https://dx.doi.org/10.1021/acs.nanolett.0c02733
Nano Lett. XXXX, XXX, XXX−XXX